

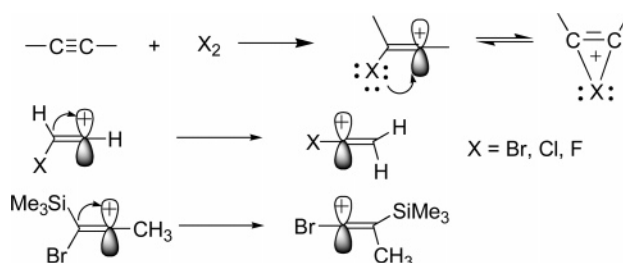
Probing the Intermediates of Halogen Addition to Alkynes:  
Bridged Halonium versus Open Halovinyl Cation;  
A Theoretical Study

Takao Okazaki<sup>†,‡</sup> and Kenneth K. Laali<sup>\*,†</sup>

Department of Chemistry, Kent State University, Kent, Ohio 44242, and Department of Energy and Hydrocarbon Chemistry, Graduate School of Engineering, Kyoto University, Nishikyo-ku, Kyoto 615-8510, Japan

klaali@kent.edu

Received April 27, 2005



Intermediates formed in halogen addition (X = Br, Cl, F) to alkynes (ethyne, propyne, 2-butyne, trifluoromethylethyne, trimethylsilylethyne, and 1-trimethylsilylpropyne) were studied computationally by MP2 at the MP2/6-311++G(3df,3pd) level and/or by DFT at the B3LYP/6-31+G(d) level. Structure optimization and frequency calculations were performed to identify the minima and to obtain their relative energies. PCM calculations (with H<sub>2</sub>O, CH<sub>2</sub>Cl<sub>2</sub>, and CCl<sub>4</sub> as model solvents) were employed to examine solvation effects on the relative stabilities in the resulting bridged halonium,  $\beta$ -halovinyl, or  $\alpha$ -halovinyl cations. GIAO-MP2 and GIAO-DFT calculations were employed to compute NMR chemical shifts (<sup>13</sup>C, <sup>19</sup>F, and <sup>29</sup>Si as appropriate). In selected cases, PCM-GIAO calculations were also performed to investigate the extent of solvent effects on the computed NMR shifts. The NPA-derived charges and the GIAO shifts were examined in comparative cases to shed light on structural features. In several cases, structure optimization starting with the  $\beta$ -halovinyl cations resulted in  $\alpha$ -halovinyl cations (via formal hydride shift or trimethylsilyl shift). With the CF<sub>3</sub> derivative (when X = F), a formal F shift results in polyfluoroallyl cation generation from fluorovinyl cation as starting geometry.

## Introduction

In halogenation of alkenes, formation of  $\beta$ -halocarbo-cations **a** or ethylenehalonium ions **b** and their interplay (Figure 1a) is a well-investigated classical “organic textbook” problem.<sup>1</sup> Apart from kinetics and stereochemical studies, a relatively large number of cyclic halonium

ions (type **b**) were generated by Olah and associates from suitable precursors under stable ion conditions and studied directly by NMR techniques; some were found to be in equilibrium with the open  $\beta$ -halocarbo-cations (type **a**), and others could be isolated as stable salts.<sup>2–4</sup>

The structural/mechanistic aspects of alkene bromination were discussed in a detailed review by Ruasse.<sup>5</sup> Damrauer, Leavall, and Hadad<sup>6</sup> reported a theoretical

\* To whom correspondence should be addressed. Phone: 330-672-2988. Fax: 330-672-3816.

<sup>†</sup> Kent State University.

<sup>‡</sup> Kyoto University.

(1) (a) Carey, F. A.; Sundberg, R. J. *Advanced Organic Chemistry*, 4th ed.; Kluwer Academic/Plenum Publishers: New York, 2000; Part A, Chapter 6. (b) Carroll, F. A. *Perspectives on Structure and Mechanism in Organic Chemistry*; Brooks/Cole: Pacific Grove, CA, 1998; Chapter 9. (c) Isaacs, N. S. *Physical Organic Chemistry*, 2nd ed.; Longman Scientific & Technical: Essex, U.K., 1995; Chapter 12. (d) Lowry, T. H.; Richardson, K. S. *Mechanism and Theory in Organic Chemistry*, 3rd ed.; Harper: New York, 1987; Chapter 7.

(2) Olah, G. A.; Laali, K. K.; Wang, Q.; Prakash, G. K. S. *Onium Ions*; Wiley: New York, 1998; Chapter 6.

(3) Olah, G. A. *Halonium Ions*; Wiley: New York, 1975.

(4) Olah, G. A.; Prakash, G. K. S.; Sommer, J. *Superacids*; Wiley: New York, 1985; Chapter 4.

(5) Ruasse, M.-F. In *Advances in Physical Organic Chemistry*; Bethel, D., Ed.; Academic Press: New York, 1993; Vol. 28, pp 207–291.

(6) Damrauer, R.; Leavall, M. D.; Hadad, C. M. *J. Org. Chem.* **1998**, *63*, 9476.

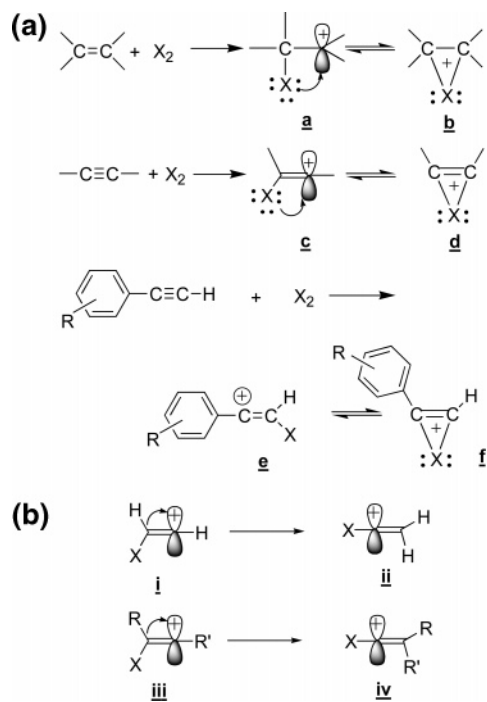


**FIGURE 1.** (a) Mechanism for reactions of alkene and alkyne with halogens. (b) Rearrangement of  $\beta$ -halovinyl cations to  $\alpha$ -halovinyl cations.

study of cyclopentene and cyclohexene halonium ions. In comparison, a limited number of studies have dealt with halogenation of alkynes as a means to access  $\beta$ -halovinyl cation **c** and/or the unsaturated cyclic (bridged) halonium ion **d**.<sup>7</sup> Kinetic studies and product analysis indicated vinyl cation–chloride ion pair formation in chlorination of terminal and disubstituted alkynes.<sup>7</sup> The open vinyl cation is also the likely intermediate in bromination of phenylacetylenes.<sup>7</sup> The Ad<sub>E</sub>3 mechanism has been invoked in the presence of added salt (LiBr). On the other hand, predominant formation of the *anti*-dibromo adducts and absence of *syn* or solvent-incorporated products suggested that **d** should be a key intermediate.<sup>7</sup> In bromination of ring-substituted 3-arypropynes, depending on R, either a cyclic phenonium ion or a cyclic bromirenium (bridged halonium) ion is formed, resulting in predominant formation of the *syn*- and *anti*-dibromides, respectively.<sup>7</sup> It has been stated that alkynes with alkyl substituents at the triple bond are more likely to go through a cyclic onium ion **d**, whereas phenylacetylenes would go through the open vinyl cation **e**, with the tendency for cyclization increasing in the order I > Br > Cl (corresponding to the bridging ability of halogens).<sup>1b,7</sup> Chiappe et al.<sup>8a</sup> showed that bromination of alkynes with Br<sub>2</sub> in [BMIM][Br] ionic liquid is *anti*-stereospecific irrespective of the nature of substituents at the triple bond, whereas the same reaction in [BMIM][PF<sub>6</sub>] gave *syn/anti* mixtures. On the basis of kinetic studies,<sup>8b</sup> involvement of an open vinyl cation (type **c** in Figure 1a)

(7) (a) Stang, P. J.; Rappoport, Z.; Hanack, M.; Subramanian, L. R. *Vinyl Cations*; Academic Press: New York, 1979. (b) Luchini, V.; Modena, G.; Pasquato, L. In *Dicoordinated Carbocations*; Rappoport, Z., Stang, P. J., Eds.; Wiley: New York, 1997; Chapter 6.

(8) (a) Chiappe, C.; Capraro, D.; Conte, V.; Pieraccini, D. *Org. Lett.* **2001**, *3*, 1061. (b) Chiappe, C.; Conte, V.; Pieraccini, D. *Eur. J. Chem.* **2002**, 2831.

was invoked in bromination of PhC≡CR and a bridged bromirenium ion (type **d**, Figure 1a) in the case of *p*-CF<sub>3</sub>-PhC≡CR in [BMIM][PF<sub>6</sub>] solvent.<sup>8b</sup>

Bromination of alkynylsilanes including HC≡CTMS with Br<sub>2</sub> in CCl<sub>4</sub> under mild conditions was reported to produce the corresponding *anti*-dibromovinylsilanes.<sup>9</sup>

A number of long-lived vinyl cations, in particular the  $\beta$ -silyl-stabilized analogues, have been generated under stable ion conditions mainly by protonation of suitably substituted alkynes. Authoritative progress reviews on the topic by Siehl<sup>10a,b</sup> and by Siehl and Müller<sup>10c</sup> are available.

To our knowledge, there are as yet no examples of bridged halonium ions of types **d** and **f** (Figure 1a) as NMR observable species. Similarly, for the open vinyl cations, despite an impressive literature on persistent vinyl cations,<sup>10</sup> no examples seem to exist for  $\beta$ -halovinyl cations of type **i** or **iii** (Figure 1b) nor on  $\alpha$ -halovinyl cations as in **ii** or **iv** (Figure 1b), and no extensive theoretical studies are available to serve as guide to their relative stabilities ( $\beta$ -halovinyl versus  $\alpha$ -halovinyl) and possible interconversion as a function of halogen and cation structure.

Parent vinyl cation (protonated acetylene) itself is predicted to be bridged (as in **d** with X = H).<sup>11</sup> A theoretical study on the C<sub>2</sub>H<sub>2</sub>F<sup>+</sup> cation was reported,<sup>12</sup> showing that the cyclic ion is a transition state and the open  $\beta$ -fluorovinyl cation is 31 kcal/mol lower in energy. The importance of polarization functions and electron correlation has been emphasized by Hamilton and Schaefer for the C<sub>2</sub>H<sub>2</sub>Cl<sup>+</sup> and C<sub>2</sub>H<sub>2</sub>Br<sup>+</sup> cations,<sup>13</sup> illustrating that at the more advanced levels the open halovinyl cations become shallow minima or transition states. Recent progress in high level theoretical studies of vinyl cations and their isomers, including C<sub>2</sub>H<sub>2</sub>X<sup>+</sup> ions, has been discussed in a review by Apeloig and Müller,<sup>14a</sup> and more recent computational studies have been reported by van Alem, Lodder, and Zuilhof.<sup>14b,c</sup>

In an effort to obtain a more comprehensive picture as to the relative stabilities of halogen cations **c** versus **d**, and **i/iii** versus **ii/iv** as a function of alkyne structure and the nature of halogen, we performed an extensive theoretical study by DFT and MP2 methods, focusing on the bridged halonium ions and the open vinyl cations formed when halogens (X = Br, Cl, F) react with ethyne, propyne, 2-butyne, trifluoromethylethyne, trimethylsilylethyne and 1-trimethylsilylpropyne. The influence of solvation (in CH<sub>2</sub>Cl<sub>2</sub>, CCl<sub>4</sub>, and H<sub>2</sub>O) on the relative

(9) Al-Hassan, M. I. *J. Organomet. Chem.* **1989**, *372*, 183.

(10) (a) Siehl, H.-U. In *Stable Carbocation Chemistry*; Prakash, G. K. S., Schleyer, P. v. R., Eds.; Wiley: New York, 1997; Chapter 5. (b) Siehl, H.-U. In *Dicoordinated Carbocations*; Rappoport, Z., Stang, P. J., Eds.; Wiley: New York, 1997; Chapter 5. (c) Siehl, H.-U.; Müller, T. In *The Chemistry of Organic Silicon Compounds*; Rappoport, Z., Apeloig, Y., Eds.; Wiley: Chichester, 1998; Vol. 2, Part 1, Chapter 12.

(11) (a) Weber, J.; Yoshimine, M.; McLean, A. D. *J. Chem. Phys.* **1976**, *64*, 4159. (b) Lindh, R.; Rice, J. E.; Lee, T. J. *J. Chem. Phys.* **1991**, *94*, 8008.

(12) Csizmadia, I. G.; Luchini, U.; Modena, G. *Theor. Chim. Acta* **1975**, *39*, 51.

(13) Hamilton, T. P.; Schaefer, H.-F., III. *J. Am. Chem. Soc.* **1991**, *113*, 7147.

(14) (a) Apeloig, Y.; Müller, T. In *Dicoordinated Carbocations*; Rappoport, Z., Stang, P. J., Eds.; Wiley: New York, 1997; Chapter 2. (b) van Alem, K.; Lodder, G.; Zuilhof, H. *J. Phys. Chem. A* **2000**, *104*, 2780. (c) van Alem, K.; Lodder, G.; Zuilhof, H. *J. Phys. Chem. A* **2002**, *106*, 10681.

stabilities of the two types of intermediates was probed in selected cases via the PCM method. The GIAO-derived NMR chemical shifts and the NPA-derived charges were computed for the resulting minima. In selected cases, solvent effects were also examined on the NMR chemical shifts and on charge distribution. It was hoped that the collective data would help with the design of experiments that could lead to direct observation and NMR study of the cyclic cations of type **d** and/or halovinyl cations of types **i–iv**.

## Results and Discussion

**Computational Protocols.** Structures were optimized using molecular point groups shown in Tables 1 and S2–7 (Supporting Information) by the density functional theory (DFT) method at B3LYP/6-31+G(d) level and the Møller–Plesset perturbation theory at MP2/6-311++G(3df,3pd) level using the Gaussian 03 package.<sup>15</sup> Solvent effects were included using the polarizable continuum model (PCM),<sup>16</sup> and the dielectric constants of 78.39, 8.93, and 2.228 were used for H<sub>2</sub>O, CH<sub>2</sub>Cl<sub>2</sub>, and CCl<sub>4</sub>. Computed geometries were verified by frequency calculations. Furthermore, global minima were checked by manually changing initial geometries and by comparing the resulting optimized structures and their energies. NMR chemical shifts were calculated by the gauge-including atomic orbital (GIAO)<sup>17,18</sup> method at the B3LYP/6-31+G(d)/B3LYP/6-31+G(d) or the MP2/6-311++G(3df,3pd)/MP2/6-311++G(3df,3pd) level. NMR chemical shifts were referenced to CH<sub>3</sub>F for  $\delta^{13}\text{C}$  (71.6 ppm) and  $\delta^{19}\text{F}$  (–271.9 ppm) and to TMS for  $\delta^{29}\text{Si}$  (0 ppm) calculated with a molecular symmetry of  $C_{3v}$  or  $T_d$  at the same level of theory (Table S1). At the onset, GIAO-derived isotropic magnetic shielding tensors were calculated for CH<sub>4</sub>, MeF, Me<sub>4</sub>Si, CCl<sub>3</sub>F, C<sub>6</sub>H<sub>6</sub>, and C<sub>6</sub>F<sub>6</sub> by B3LYP/6-31+G(d) and for CH<sub>4</sub> and MeF at the MP2/6-311++G(3df,3pd) level. As Table S3 illustrates, the computed values obtained for these reference compounds were in good overall agreement with their reported experimental values, except for CCl<sub>3</sub>F, whose GIAO-derived  $\delta^{13}\text{C}$  deviated noticeably from the reported experimental value. On the basis of these “inter-referencing” tests (Table S1), MeF was selected for calibration and refer-

encing of the GIAO-derived <sup>13</sup>C and <sup>19</sup>F NMR chemical shifts at both MP2 and DFT levels (see earlier discussion).

As a test of basis-set dependency of GIAO chemical shifts,<sup>17</sup> the bridged cations **1Br** and **1Cl**, the  $\beta$ -halovinyl cation **2F**, and the  $\alpha$ -halovinyl cations **3Br**, **3Cl**, and **3F** (see later discussion) were computed at various DFT and MP2 levels. The data are summarized in Figure S1a. It can be seen that the largest changes are for the C<sup>+</sup> centers in the vinyl cations, with the MP2-derived shifts being less deshielded than those from DFT. For the bridged halonium ions, the variations are less significant, with the MP2-derived values being smaller. These tests indicated that the employed levels were adequate, especially for comparative purposes to derive trends.

Tables 1 and S2–7 (in Supporting Information) summarize the total electronic energies ( $E$ ), zero point energies (ZPE), and relative energies ( $\Delta E$ ) for the studied compounds. Natural population analysis (NPA)-derived charges were computed at the same levels.

**Reactive Intermediates of Halogenation of Ethyne; the C<sub>2</sub>H<sub>2</sub>X<sup>+</sup> Cations.** Although relative energies and geometries for the C<sub>2</sub>H<sub>2</sub>X<sup>+</sup> ions had previously been computed at the correlated levels and were discussed in ref 13, solvent effects and computed NMR chemical shifts were not available. Siehl and associates<sup>19</sup> examined the influence of basis set on computed NMR chemical shifts for several  $\alpha$ -vinyl-substituted vinyl cations (dienyl cations). The closest values to experimental NMR values were obtained at correlated levels [MP2 and CCSD(T)], whereas HF-SCF calculations were unsatisfactory.

More recently, Müller and co-workers<sup>20</sup> reported a reasonable linear correlation between experimental and computed <sup>13</sup>C NMR chemical shifts by GIAO-DFT in a series of  $\alpha$ -aryl- $\beta$ -disilyl-substituted vinyl cations.

Our study began with a reexamination of C<sub>2</sub>H<sub>2</sub>X<sup>+</sup> ions (i.e., the reactive intermediates of halogen addition to parent acetylene).

Results of  $E$ , ZPE, and  $\Delta E$  for the derived cyclic halonium ions and the vinyl cations are summarized in Table 1 along with their molecular symmetry. The cyclic bromonium **1Br** and cyclic chloronium **1Cl** ions are minima ( $C_{2v}$  symmetry) at both B3LYP/6-31+G(d) and MP2/6-311++G(3df,3pd) levels (Figure 2). The cyclic fluoronium ion **1F** is minimum at the MP2/6-311++G(3df,3pd) level and a transition state (TS) at the B3LYP/6-31+G(d) level (**1F** was found to be a TS at the MP3/6-31G\*\*/6-31G\* level).<sup>14a</sup>

Focusing on the open vinyl cations, we found that the  $\beta$ -bromo **2Br** and the  $\beta$ -chlorovinyl cations **2Cl** did not exist as stable species (see later discussion), but the  $\beta$ -fluorovinyl cation **2F** is minimum. Geometry optimization on **2Br** and **2Cl** as starting geometries resulted in rearrangement (a formal hydride shift) to produce the corresponding  $\alpha$ -halovinyl cations **3Br** and **3Cl**, which are minima at both B3LYP/6-31+G(d) and MP2/6-311++G(3df,3pd) levels.

(15) Frisch, M. J.; Trucks, G. W.; Schlegel, H. B.; Scuseria, G. E.; Robb, M. A.; Cheeseman, J. R.; Montgomery, J. A., Jr.; Vreven, T.; Kudin, K. N.; Burant, J. C.; Millam, J. M.; Iyengar, S. S.; Tomasi, J.; Barone, V.; Mennucci, B.; Cossi, M.; Scalmani, G.; Rega, N.; Petersson, G. A.; Nakatsuji, H.; Hada, M.; Ehara, M.; Toyota, K.; Fukuda, R.; Hasegawa, J.; Ishida, M.; Nakajima, T.; Honda, Y.; Kitao, O.; Nakai, H.; Klene, M.; Li, X.; Knox, J. E.; Hratchian, H. P.; Cross, J. B.; Adamo, C.; Jaramillo, J.; Gomperts, R.; Stratmann, R. E.; Yazyev, O.; Austin, A. J.; Cammi, R.; Pomelli, C.; Ochterski, J. W.; Ayala, P. Y.; Morokuma, K.; Voth, G. A.; Salvador, P.; Dannenberg, J. J.; Zakrzewski, V. G.; Dapprich, S.; Daniels, A. D.; Strain, M. C.; Farkas, O.; Malick, D. K.; Rabuck, A. D.; Raghavachari, K.; Foresman, J. B.; Ortiz, J. V.; Cui, Q.; Baboul, A. G.; Clifford, S.; Cioslowski, J.; Stefanov, B. B.; Liu, G.; Liashenko, A.; Piskorz, P.; Komaromi, I.; Martin, R. L.; Fox, D. J.; Keith, T.; Al-Laham, M. A.; Peng, C. Y.; Nanayakkara, A.; Challacombe, M.; Gill, P. M. W.; Johnson, B.; Chen, W.; Wong, M. W.; Gonzalez, C.; Pople, J. A. *Gaussian 03*, revision B.05; Gaussian, Inc.: Pittsburgh, PA, 2003.

(16) Tomasi, J.; Persico, M. *Chem. Rev.* **1994**, *94*, 2027.

(17) (a) Wolinski, K.; Hinton, J. F.; Pulay, P. *J. Am. Chem. Soc.* **1990**, *112*, 8251. (b) Dichfield, R. *Mol. Phys.* **1974**, *27*, 789.

(18) Wolfram, K.; Holthausen, M. C. *A Chemist's Guide to Density Functional Theory*, 2nd ed.; Wiley-VCH: Weinheim, Germany, 2000; Chapter 11.

(19) (a) Siehl, H.-U.; Müller, T.; Gauss, J. *J. Phys. Org. Chem.* **2003**, *16*, 577. (b) Siehl, H.-U.; Brixner, S. *J. Phys. Org. Chem.* **2004**, *17*, 1039.

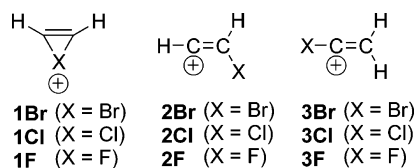
(20) Müller, T.; Margraf, D.; Syha, Y. *J. Am. Chem. Soc.* **2005**, *127*, 10852.



**TABLE 1.** Electronic Energies ( $E$ ), Zero Point Energies (ZPE), and Relative Energies ( $\Delta E$ ) for **1Br**, **3Br**, **1Cl**, **2Cl**, **3Cl**, **1F**, **2F**, and **3F** by MP2/6-311++G(3df,3pd) and/or by B3LYP/6-31+G(d)

cation	method	molecular point group	$E$ , hartree	ZPE hartree	no. of imaginary frequencies	$\Delta E$ , <sup>a</sup> kcal/mol
<b>1Br</b>	B3LYP/6-31+G(d)	$C_{2v}$	-2648.7079359	0.028262	0	(0)
	MP2/6-311++G(3df,3pd)	$C_{2v}$	-2649.3565994	0.028422	0	(0)
<b>3Br</b>	B3LYP/6-31+G(d)	$C_s$	-2648.7426163	0.028713	0	-21.8
	MP2/6-311++G(3df,3pd)	$C_{2v}$	-2649.3712008	0.028006	0	-9.2
<b>1Cl</b>	B3LYP/6-31+G(d)	$C_{2v}$	-537.1667424	0.028519	0	(0)
	MP2/6-311++G(3df,3pd)	$C_{2v}$	-536.5005387	0.028913	0	(0)
<b>2Cl</b>	B3LYP/6-31+G(d)	$C_s$	-537.1586864	0.027511	1	5.1
<b>3Cl</b>	B3LYP/6-31+G(d)	$C_s$	-537.2050724	0.028714	0	-24.1
		$C_{2v}$	-537.2050724	0.028715	0	-24.1
<b>1F</b>	MP2/6-311++G(3df,3pd)	$C_{2v}$	-536.5299165	0.028727	0	-18.4
	B3LYP/6-31+G(d)	$C_{2v}$	-176.7550981	0.028703	1	(0)
	MP2/6-311++G(3df,3pd)	$C_{2v}$	-176.4569861	0.028844	0	(0)
<b>2F</b>	B3LYP/6-31+G(d)	$C_s$	-176.7793393	0.028758	0	-15.2
<b>3F</b>	B3LYP/6-31+G(d)	$C_{2v}$	-176.8177664	0.029891	0	-39.3
	MP2/6-311++G(3df,3pd)	$C_{2v}$	-176.5200878	0.029783	0	-39.6

<sup>a</sup> Relative energy ( $\Delta E$ ) compared to bridged cations, **1Br**, **1Cl**, and **1F**, at the same level.

**FIGURE 2.** Intermediates of halogen addition to acetylene.

The rearranged open vinyl cation **3Br** is strongly favored relative to the cyclic ion **1Br** (by 21.8 kcal/mol at the B3LYP/6-31+G(d) level and by 9.2 kcal/mol at the MP2/6-311++G(3df,3pd) level; an energy difference of 13.8 kcal/mol was computed at the CISD(+Q)/DZ+d//CISD/DZ+d level).<sup>14a</sup> Similarly, the rearranged open vinyl cation **3Cl** is more stable than the bridged ion **1Cl** (by 24.1 kcal/mol at the B3LYP/6-31+G(d) level and by 18.4 kcal/mol at the MP2/6-311++G(3df,3pd) level; the difference was computed to be 20.6 kcal/mol by MP4/6-311G(2df,p)/MP2/6-311G\*\*+ZPE+ thermal energy).<sup>14a</sup> Whereas the  $\beta$ -fluorovinyl cation **2F** and the  $\alpha$ -fluorovinyl cation **3F** are both minima at the B3LYP/6-31+G(d) level, **3F** is noticeably more stable.

Overall, in agreement with previous findings included in ref 14a, from an energetic standpoint, the  $\alpha$ -halovinyl cations are the preferred intermediates in halogen addition to acetylene, but the relative importance of bridged halonium ion **1Br** and to a lesser extent **1Cl** should not be overlooked.

The GIAO-derived <sup>13</sup>C NMR chemical shifts and the NPA-derived charges for the cyclic halonium ions **1Br**, **1Cl**, and **1F**, and for the open vinyl cations **3Br**, **3Cl**, **2F**, and **3F** were computed at the MP2/6-311++G(3df,3pd) and/or B3LYP/6-31+G(d) level. These data along with the optimized structures are summarized in Figure S1.

The NPA-derived charges indicate that positive charge in **1Br** and **1Cl** resides on the halogens. In the fluoronium ion **1F**, positive charge resides on the carbons, and fluorine bears negative charge. This trend is reflected in the computed <sup>13</sup>C GIAO chemical shifts, which show a deshielding trend in the order **1F** > **1Cl** > **1Br**. Computed  $\delta$  <sup>13</sup>C for the bridged bromonium ion **1Br** is 90.5 ppm (by B3LYP) and 86.0 ppm (by MP2). The  $\delta$  <sup>13</sup>C for

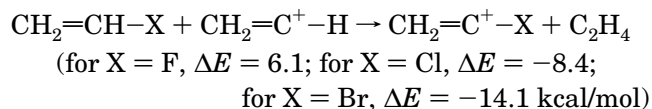
the bridged chloronium ion **1Cl** is 101.9 ppm (by B3LYP) and 96.6 ppm (by MP2), and the GIAO-derived  $\delta$  <sup>13</sup>C for the bridged fluoronium ion **1F** is 174.2 ppm (by MP2).

The bridged cations **1Br**, **1Cl**, and **1F** are symmetrical with nearly identical C–C bond lengths and with the C–X bonds changing from 2.01 Å (C–Br) to 1.86 Å (C–Cl) to 1.56 Å (C–F) (by MP2; see Figure S1).

Cyclic halonium ions are regarded as n-electron bridged species. NBO analysis indicated no 3-center bonding in **1Br**, **1Cl**, **2Cl** (this is a TS), and **1F** (also a TS) at the B3LYP/6-31+G(d) level. On the contrary, a 3-center bond is implied in **2F** for H(1)–C(1)–C(2). The H(1) atom is bonded to the cationic carbon at the optimized geometry, and the H(1)–C(1)–C(2) angle is 104.4°.

Focusing on the GIAO NMR data (in Figure S1), we see that the  $\beta$ -fluorovinyl cation **2F** has an unusually deshielded C<sup>+</sup> (at 453 ppm) and a shielded  $\delta$ <sup>19</sup>F (at –260 ppm) by B3LYP as compared to  $\alpha$ -fluorovinyl cation **3F** whose C<sup>+</sup> is at 242 ppm and  $\delta$ <sup>19</sup>F at 81 ppm by MP2. This trend presumably reflects significant fluoronium ion character in **3F** by p- $\pi$  back-bonding. The computed <sup>13</sup>C NMR chemical shift for the C<sup>+</sup> in **3F** (242.8 ppm) is in close range of the experimental value for Mes-C<sup>+</sup>=CH<sub>2</sub> reported at 238.5 ppm.<sup>10b</sup>

GIAO-derived  $\delta$ <sup>13</sup>C values for **3Br** are at 311.0 (Br–C<sup>+</sup>) and 65.9 ppm (CH<sub>2</sub>) by B3LYP, and at 287.9 (Br–C<sup>+</sup>) and 66.7 ppm (CH<sub>2</sub>) by MP2. For **3Cl** these are at 296.7 (Cl–C<sup>+</sup>) and 54.8 ppm (CH<sub>2</sub>) by B3LYP, and at 274.2 (Cl–C<sup>+</sup>) and 54.6 (CH<sub>2</sub>) by MP2. Comparing these data with those of **3F** reveals a shielding trend on both the vinylic carbocation center and the CH<sub>2</sub> in the order Br < Cl < F, which correlates with the back-bonding ability of halogens in  $\alpha$ -halocarbenium ions.<sup>21</sup> But at the same time, consideration of the energetics of isodesmic reaction below (MP3 or CISD calculations)<sup>14</sup> leads one to conclude that destabilization by  $\sigma$ -withdrawal versus stabilization by p- $\pi$  back-bonding is largest for X = F and smallest for X = Br.



**Solvent Effect on Relative Stabilities; PCM Calculations for  $C_2H_2X^+$  Cations.** To gather some insight into solvation effects on relative stabilities of the open versus cyclic cations, the cyclic halonium ions **1Br**, **1Cl**, **1F** and the halovinyl cations **3Br**, **3Cl**, **2F**, and **3F** were re-optimized in  $H_2O$ ,  $CH_2Cl_2$ , and  $CCl_4$  as solvent using the PCM method. The data are summarized in Table S2. It can be seen that solvent has a significant energy lowering effect on the cations in the order  $H_2O > CH_2Cl_2 > CCl_4$ . Among the bridged halonium ions, the stabilization order **1F** > **1Cl** > **1Br** is observed. Geometry optimization on **2F** ( $\beta$ -fluorovinyl cation) in water afforded **3F** ( $\alpha$ -fluorovinyl cation) as the final geometry. As Table S2 illustrates, vinyl cations are also strongly stabilized by solvation, but to a lesser extent as compared to their cyclic counterparts. These model PCM calculations imply that bridged halonium ions  $C_2H_2X^+$  enjoy significant stabilization in solution, and this underscores their relevance in solution studies.

There are no notable changes in the optimized structures and in the NPA charges in the bridged cations or the vinyl cations when solvation effects are implemented (Figure S2). There are only small changes in the GIAO- $\delta^{13}C$  values, and the resulting changes are in the order  $H_2O > CH_2Cl_2 > CCl_4$ , which corresponds to the dielectric constants. Whereas the GIAO  $^{13}C$  chemical shifts for **1Br** and **1Cl** are only slightly affected by solvent, magnitude of positive charge at halogen is diminished in the order  $H_2O > CH_2Cl_2 > CCl_4$ , according to the polarities.

Whereas solvent effects on  $^{13}C$  chemical shift changes in the  $\alpha$ -halovinyl cations **3Br**, **3Cl**, and **3F** are relatively small, large changes were computed for the  $\beta$ -fluorovinyl cation **2F** between  $CH_2Cl_2$  and  $CCl_4$  (geometry optimization on **2F** in  $H_2O$  afforded **3F**).

**Reactive Intermediates of Halogenation of Propyne; the  $C_2H(Me)X^+$  Cations.** Upon structure optimizations at the B3LYP/6-31+G(d) level, bridged halonium ions derived from propyne (**4Br**, **4Cl**, **4F** and **4aBr**, **4aCl**, **4aF**) converged to open vinyl cations (**5Br**, **5Cl**, **5F** and **5aBr**, **5aCl**, **5aF**) (Figure 3).

The energy data for the gas phase as well as those calculated by the PCM method in  $H_2O$ ,  $CH_2Cl_2$ , and  $CCl_4$  as representative solvents are gathered in Table S3 for comparison. For **5Br**, PCM calculations in  $H_2O$  and  $CH_2Cl_2$  gave structures with one imaginary frequency, whereas all other structures were minima in all solvents.

PCM calculations indicate a stabilization trend for this group similar to those found for **3Br**, **3Cl**, and **3F** (i.e.,  $H_2O > CH_2Cl_2 > CCl_4$ ) (Table S3).

For comparison, the corresponding  $\alpha$ -halovinyl cations, **6Br**, **6Cl**, and **6F** were also calculated and found to be minima (Table S3). Whereas **6Br** and **6Cl** are more stable than **5Br** and **5Cl** (by 8.3 and 4.7 kcal/mol, respectively), **6F** is less stable than **5aF** (by 1.9 kcal/mol). Species **6aBr**, **6aCl**, and **6aF** were found to be transition states to methyl rotation in **6Br**, **6Cl**, and **6F**.

On the basis of these findings, the  $\beta$ -halovinyl and the  $\alpha$ -halovinyl cations are both minima in halogenations of propyne (these vinyl cations are readily interconvertible via 1,2-H shifts), and no bridged cations were obtained as final structures at this level.

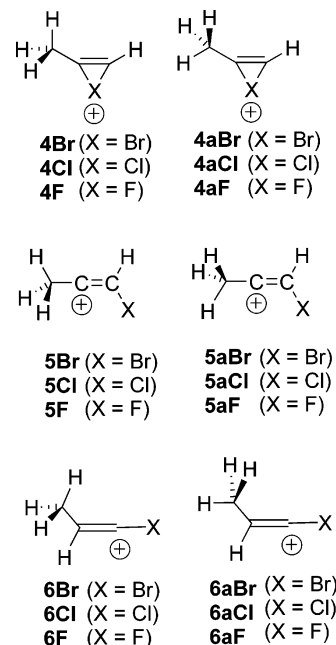


**FIGURE 3.** Halonium ions and vinyl cations by halogen addition to propyne.

GIAO-derived NMR chemical shifts, NPA-derived charges, and geometries for the  $\beta$ -halovinyl cations derived from propyne are summarized in Figure S3, whereas data for the  $\alpha$ -halovinyl cations are summarized in Figure S3a.

For the  $\beta$ -halovinyl cations (**5Br**, **5Cl**, and **5aF**), the GIAO- $\delta^{13}C$  values at the vinylic carbocation (and the CHX) follow the order  $Br < Cl < F$ , but the reverse order is observed in the  $\alpha$ -halovinyl cations (**6Br**, **6Cl**, and **6F**).

The NPA charge at the vinylic carbocation in the  $\beta$ -halovinyl cations are computed to be 0.404 (for **5Br**), 0.478 (for **5aBr**), 0.502 (for **5Cl**), 0.506 (for **5aCl**), 0.458 (for **5F**), and 0.442 (for **5aF**), and these values decrease in the order  $H_2O > CH_2Cl_2 > CCl_4$ . For the  $\alpha$ -halovinyl cations, the NPA-derived charges at the vinylic carbocations are 0.108 (in **6Br**), 0.228 (in **6Cl**), and 0.885 (in **6F**).

The dihedral angles for  $H-C(3)-C(1)-X$  are  $180^\circ$  in **5Br**, **5Cl**, and **5F** and  $0^\circ$  in **5aBr**, **5aCl**, and **5aF**, and based on relative energies the former group (with the exception of **5F**) is slightly more stable. In the optimized structures, the vinylic moiety ( $C/C$  double bond) becomes longer and the  $Me-C$  bond becomes shorter in the sequence  $F > Cl > Br$  (Figure S3).

NBO analysis for **5Cl** and **5aF** implies a 3-center bonding in  $C(2)-C(3)-H(3)$ , with a bond angle of less than  $120^\circ$ .

**Reactive Intermediates of Halogenation of 2-Butyne; the  $(Me)_2C_2X^+$  Cations.** The bridged halonium ions and the open vinyl cations shown in Figure 4 were computed by DFT, and energies of their optimized structures are summarized in Table S4. Among the bridged cations (Figure 4), **7Br**, **7Cl**, and **7F** had the lowest energies, but frequency analysis indicated that they were transition states (one imaginary frequency) to the formation of the  $\beta$ -halovinyl cations **8Br**, **8Cl**, **8cCl**, and **8cF**, which were minima (had no imaginary fre-

(21) Olah, G. A.; Mo, Y. K.; Halpern, Y. *J. Am. Chem. Soc.* **1972**, *94*, 3551.

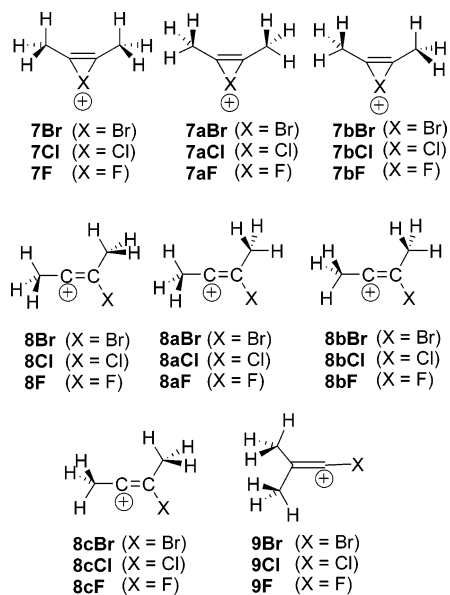


**FIGURE 4.** Halonium ions and vinyl cations as intermediates in halogen addition to 2-butyne.

quency). Geometry optimization on **7bBr** (included in Figure 4) as initial structure resulted in **8cBr** as the final structure.

The  $\alpha$ -halovinyl cations **9Br**, **9Cl**, and **9F** are formed by methyl migration via **8Br**, **8Cl** (or **8cCl**), and **8cF**. Whereas energies of **9Br** versus **8Br** and **9Cl** versus **8Cl** are rather close (marginally favoring the  $\alpha$ -halovinyl cation), in the case of fluorinated vinyl cations the  $\beta$ -fluoro analogue **8cF** is strongly preferred relative to  $\alpha$ -fluorovinyl cation **9F** (by 8.3 kcal/mol).

Their GIAO-derived NMR chemical shifts, NPA-derived charges, and the optimized structures with bond lengths are summarized in Figure S4.

Computed GIAO- $\delta^{13}\text{C}$  values for the vinylic carbocation (and the CHX carbon) at the cationic centers increase in the order  $\text{F} > \text{Cl} > \text{Br}$  in the  $\beta$ -halovinyl cations (**8Br**, **8Cl**, **8cCl**, and **8cF**), while the opposite trend is seen in the  $\alpha$ -halovinyl cations (**9Br**, **9Cl**, and **9F**) (Figure S4). Comparison of the GIAO shifts in  $\alpha$ -halovinyl cations **3X**, **6X**, and **9X** (X = Br, Cl, and F) indicates fairly regular methyl substituent effects. But methyl substitution in the  $\beta$ -halovinyl cations **5X** and **8X** induces dramatic shielding effect on the vinylic cation centers, in the case of X = Br and X = Cl, but little effect is seen when X = F. Inspection of the X-C=C angles ( $100.3^\circ$  for **5Br**,  $119.1^\circ$  for **5Cl**,  $124.1^\circ$  for **5aF**,  $89.3^\circ$  for **8Br**,  $103.1^\circ$  for **8Cl**, and  $120.9^\circ$  for **8cF**, and increasing in the order  $\text{F} > \text{Cl} > \text{Br}$ ) provides some insight, pointing to partial bridging by bromine and chlorine in the more crowded analogues as an important contributing factor to vinyl cation shielding. It is also noteworthy that in the optimized structures the C-X bond (X = Br, Cl) is elongated in **8X** relative to **5X**.

Among the  $\beta$ -fluorovinyl cations, the  $^{19}\text{F}$  chemical shift in **2F** and **5aF** are nearly the same but that in **8cF** is  $\sim 55$  ppm more downfield.

Finally, the computed NPA charge at the vinylic cation center is 0.304 (for **8Br**), 0.437 (for **8Cl**), and 0.431 (for **8cF**), which, in comparison with **5Br**, **5Cl**, and **5aF**, has diminished by 0.100 (for **8Br**), 0.065 (for **8Cl**), and 0.011 for (**8cF**).

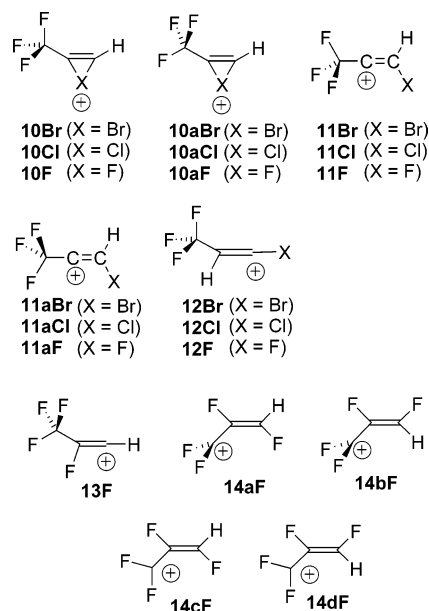


**FIGURE 5.** Halonium ions and vinyl cations intermediates in halogen addition to trifluoromethylacetylene.

**Intermediates of Halogenation of Trifluoromethylethyne;  $\text{C}_2\text{H}(\text{CF}_3)\text{X}^+$  Cations.** The bridged halonium ions (**10Br**–**10F** and **10aBr**–**10aF**) and the open vinyl cations **11Br**–**11F** and **11aBr**–**11aF** were calculated by DFT as initial structures (Figure 5), and energies of their optimized structures are summarized in Table S5.

In the case of Br-substituted cations, only the bridged species **10Br**, **10aBr**, and the rearranged vinyl cation **12Br** were obtained as final structures, and structures **11Br** or **11aBr** could not be obtained at the B3LYP/6-31+G(d) level. Frequency analyses showed that **10Br** and **12Br** are minima, but **10aBr** is a transition state for rotation of a  $\text{CF}_3$  group in **10Br**.

For the Cl-substituted cations, **10Cl**, **10aCl**, **11aCl**, and **12Cl** were obtained as optimized geometries, and frequency analyses indicated that only **10Cl**, **11aCl**, and **12Cl** are minima. It is noteworthy that in this case the bridged ion **10Cl** is more stable than the open vinyl cation **11aCl**. A notable feature for the bridged cations **10Br** and **10Cl** is that they are unsymmetrical, with the  $\text{CF}_3\text{C}-\text{X}$  bond being shorter.

For X = F, neither the bridged cation nor the open “unrearranged” vinyl cation could be obtained as optimized structures. Structure optimization resulted in rearranged species **12F**, **13F**, **14aF**–**14dF** as final structures. Among these, only **12F**, **14cF**, and **14dF** (isomeric polyfluorinated allyl cations) are minima. A 1,2-fluorine shift as found for **11F** has already been examined in  $\text{CF}_3\text{C}^+=\text{CHR}$  (R = H or Ph) computationally and experimentally.<sup>22</sup>

Their GIAO-derived NMR chemical shifts, NPA-derived charges, and optimized structures including bond lengths are gathered in Figure S5. The allylic nature of the rearranged cations **14cF** and **14dF** is clearly evident from these data, in particular deshielding at both  $\text{C}_1/\text{C}_3$  and deshielding of their fluorines (GIAO NMR). NPA

(22) (a) McAllister, M.; Tidwell, T. T.; Peterson, M. R.; Csizmadia, I. G. *J. Org. Chem.* **1991**, *56*, 575. (b) van Alem, K.; Belder, G.; Lodder, G.; Zuilhof, H. *J. Org. Chem.* **2005**, *70*, 179.



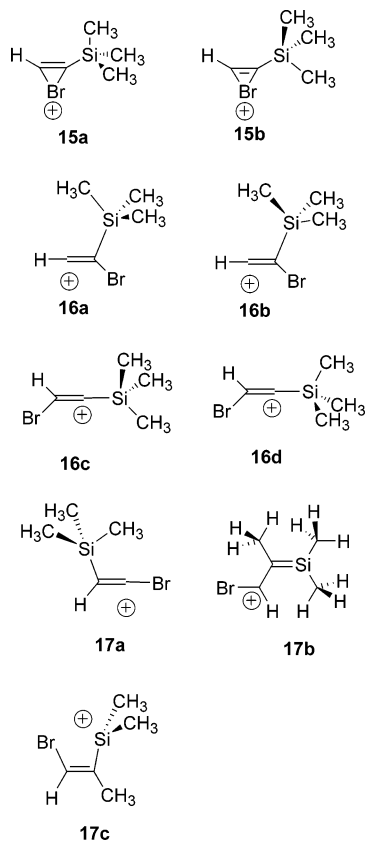


**FIGURE 6.** Halonium ions and vinyl cations intermediates in halogen addition to trimethylsilylacetylene.

charges indicate that the allylic carbocation bearing two fluorines carries significantly more positive charge relative to that having one fluorine.

Comparison between the computed GIAO NMR shifts in **1Br** and **10Br** shows that the halonium carbon attached to  $\text{CF}_3$  is more shielded relative to the unsubstituted halonium carbon, but such an effect is not implied in comparing **1Cl** with **10Cl** where the  $\text{CF}_3$  substitution appears to have little or no effect.

**Intermediates of Bromination of Trimethylsilyl-ethyne;  $\text{TMSC}_2\text{HX}^+$ .** The bridged halonium ions (**15a** and **15b**) and the open vinyl cations (**16a–d**) were calculated by DFT as initial structures (Figure 6). The bridged ion **15a**, the  $\alpha$ -bromo- $\beta$ -silylvinyl cation **17a**, and the rearranged cations **17b** and **17c** were obtained as final structures at the B3LYP/6-31+G(d) level. Frequency analyses showed that **15a** and **17a–c** are minima (energies of the optimized structures are summarized in Table S6). It is seen that the rearranged cations **17b** and **17c** and the vinyl cation **17a** are strongly preferred over **15a**. Their GIAO-derived NMR chemical shifts, NPA-derived charges, and optimized structures for **15a** and **17a–c** including bond lengths are gathered in Figure S6.

The optimized structure of **15a** shows a distorted bridged cation (as in **10Br** but more distorted), with the C–Br bond attached to the  $-\text{SiMe}_3$  group much elongated. GIAO  $^{13}\text{C}$  NMR implies that the TMS group has a notable deshielding effect on the halonium ion. Taken together, the optimized structure, NPA charges, and the GIAO  $^{29}\text{Si}$  and  $^{13}\text{C}$  shifts in **17a** (compare for example the NMR of **17a** with **6Br**) point to silicon participation

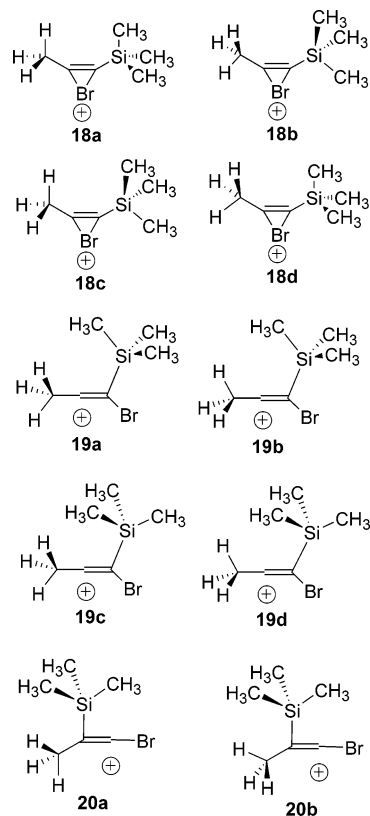


**FIGURE 7.** Cyclic bromonium ions and vinyl cations intermediates in bromine addition to 1-trimethylsilylpropyne.

and siliconium ion character in **17a**. Cation **17b** has the characteristics of a sila-allyl cation, whereas **17c** could be viewed as a silicenium species with bromonium ion character (bromine participation).

**Intermediates of Bromination of 1-Trimethylsilylpropyne;  $\text{TMSC}_2(\text{Me})\text{X}^+$ .** Structures of **18a–d**, **19a–d**, and **20b** (Figure 7) with restriction of  $C_s$  symmetry and **20a** with  $C_1$  symmetry were optimized, and their energies are summarized in Table S7. The bridged bromonium ion **18a**, the  $\beta$ -silyl-substituted  $\beta$ -bromovinyl cations **19a**, and  $\beta$ -silyl-substituted  $\alpha$ -bromovinyl cation **20a** were found to be minima by frequency calculations with a relative stability order **20a** > **19a** > **18a**. Structure **19b** was computed to be a TS for methyl rotation in **19a**, and optimization of structures **19c** and **19d** as initial structures resulted in **20a** and **20b** during optimization (TMS group migration).

GIAO-derived NMR chemical shifts, NPA-derived charges, and optimized structures including bond lengths for **18a**, **19a**, and **20a** are gathered in Figure S7.

GIAO  $^{29}\text{Si}$  shift in **19a** (81.4 ppm) is noticeably more deshielded relative to the bridged analogue **18a** (16.4 ppm), and the GIAO  $^{13}\text{C}$  for  $\text{C}^+$  in **19a** is shielded relative to that in **8Br** (144 versus 188 ppm). At the same time, the NPA charge at  $\text{C}^+$  in **19a** has diminished relative to that in **8Br** (0.211 versus 0.304). These features are consistent with silicon bridging and imply considerable siliconium ion character in **19a**. Comparison of the optimized geometries for **18a** and **19a** is also instructive, especially significant lengthening of the C–Si bond in **19a**. Formally, cation **20a** results from **19a** by a trimethylsilyl group shift. Relative orientation of the C–Si

bond in **19a** and **20a** in the optimized structures seems well-suited to silicon hyperconjugation with the vinyl cation. Comparing the geometries and the GIAO NMR data in **20a** and **17a** is also instructive. Increased positive charge at silicon in **20a** (NPA), longer C–Si and C–Br bonds and shorter C=C bond, and a more shielded vinyl cation (GIAO  $^{13}\text{C}$ ) in **20a** relative to that of **17a** imply a higher degree of silicon bridging and siliconium ion character in the more crowded vinyl cation. This feature has previously been deduced experimentally based on the NMR data in silyl-substituted dienyl cations.<sup>10b</sup>

### Comparative Discussion and Summary

Focusing first on halogenation of parent acetylene, the following key points emerge: For X = Br, both  $\alpha$ -bromovinyl cation **3Br** and the bridged bromonium ion **1Br** are minima, with the former being favored. A  $\beta$ -bromovinyl cation (**2Br**) is neither a TS nor an intermediate. For X = Cl, a similar situation holds, but the energy gap between the bridged cation **1Cl** and the  $\beta$ -chlorovinyl cation **3Cl** is now much wider.

For X = F, whereas the bridged cation **1F** is still a minimum, the difference in energy between **1F** and the  $\alpha$ -vinyl cation **3F** is so large that involvement of **1F** as an intermediate is highly unlikely. A notable difference with X = F is that **2F** (the  $\beta$ -fluorovinyl cation) is a minimum, but it is less stable relative to **3F**. It can be concluded that the energy gap between the bridged and the open cations is smallest for X = Br and largest for X = F, and this conclusion is consistent with those summarized in ref 14a (based on CISD, MP2, MP3, and MP4 calculations). Involvement of bridged halonium ions (**1Br**, **1Cl**, and even **1F**) gains further credibility via PCM calculations showing that solvation has a strong energy lowering effect on these species, and the effect is typically in the order **1F** > **1Cl** > **1Br**. The open vinyl cations are also stabilized by solvation effects but to a lesser extent, and the effects do not vary significantly as a function of X.

In halogen addition to propyne, a different picture emerges, whereby the bridged halonium ions (**4X** or **4aX**; X = Br, Cl, F) are no longer important (neither as minima nor as TS) and  $\beta$ -halovinyl cations (**5X** and or **5aX**) as well as  $\alpha$ -halovinyl cations (**6X**) emerge as key intermediates.

In halogen addition to symmetrical 2-butyne, the  $\beta$ -halovinyl cations (**8X** and/or **8aX**) appear as most likely intermediates, followed closely by the corresponding  $\alpha$ -halovinyl cations (**9X**; with X = Br and Cl), whereas the bridged analogues (**7X** or **7aX**) appear unimportant.

Replacing the methyl group in propyne for  $-\text{CF}_3$  brings about interesting outcomes depending on X. With X =

Br, the bridged cation **10Br** and the open  $\alpha$ -bromovinyl cation **12Br** are both minima, but **12Br** is significantly more stable.

With X = Cl, again both intermediates **10Cl** and **11aCl** are minima with the bridged structure **10Cl** being slightly more stable. But with X = F, neither the bridged nor the open “unrearranged” vinyl cations are minima, and skeletal rearrangement resulted in polyfluorinated allyl cations.

A comparative study of bromine addition to trimethylsilylethyne indicated that whereas the bridged halonium ion **15a** is minimum, the most likely intermediates are skeletally rearranged species (formed via formal -TMS or -Me migration) namely  $\alpha$ -bromo- $\beta$ -silylvinyl cations **17a**, **17b**, and **17c**.

Replacing a methyl in 2-butyne for a  $\text{Me}_3\text{Si}$  group brings about interesting prospects in bromine addition. Both cyclic halonium **18a** and the open  $\beta$ -bromo- $\beta$ -silylvinyl cation **19a** are minima, and the latter is more stable. A slightly more stable  $\alpha$ -bromovinyl cation (**20a**) results via a formal TMS shift.

The geometries, NPA charges, and GIAO NMR ( $^{13}\text{C}$ ,  $^{19}\text{F}$ ,  $^{29}\text{Si}$ ) data have provided insight into the structures, charge distributions, and NMR chemical shifts for the structures that were found to be minima. In general, variations in the GIAO shifts were not significantly altered when solvation effects were implemented.

The combined relative stability data and the NMR information should be helpful in designing experiments from appropriate alkynes under controlled/stable ion conditions in a search for persistent species of general type **c** and/or **d** (Figure 1a) and with structures **i–iv** (Figure 1b).

**Acknowledgment.** We are grateful to the reviewers for their careful review and for constructive comments and suggestions. This work was supported in part by the NCI of NIH (NCI 2 R15 CA07835-02A1) and by a Grant-in-Aid for Young Scientists (B) 15710160 from the Japan Society for the Promotion of Science (JSPS).

**Supporting Information Available:** Table S1: GIAO-derived isotropic magnetic shielding tensor and NMR chemical shifts for  $\text{CH}_4$ ,  $\text{CH}_3\text{F}$ , TMS,  $\text{CFCl}_3$ ,  $\text{C}_6\text{H}_6$ , and  $\text{C}_6\text{F}_6$ . Tables S2–7: Electronic energies ( $E$ ), zero point energies (ZPE), number of imaginary frequencies, and relative electronic energies ( $\Delta E$ ) obtained from DFT (or DFT/PCM) calculations. Tables S8–84: Cartesian coordinates of the optimized structures by the DFT and MP2 methods. Figures S1–7: Computed NMR chemical shifts and NPA-derived charges and optimized structures. This material is available free of charge via the Internet at <http://pubs.acs.org>.

JO050848B